
Towards Metamerism via Foveated Style Transfer

Arturo Deza

Dynamical Neuroscience
 Institute for Collaborative Biotechnologies
 UC Santa Barbara, CA, USA
 deza@dyns.ucsb.edu

Aditya Jonnalagadda

Electrical and Computer Engineering
 UC Santa Barbara, CA, USA
 aditya_jonnalagada@ece.ucsb.edu

Miguel P. Eckstein

Psychological and Brain Sciences
 Institute for Collaborative Biotechnologies
 UC Santa Barbara, CA, USA
 eckstein@psych.ucsb.edu

Abstract

Given the recent successes of deep learning applied to style transfer and texture synthesis, we propose a new theoretical framework to construct visual metamers: *a family of perceptually identical, yet physically different images*. We review work both in neuroscience related to metamer stimuli, as well as computer vision research in style transfer. We propose our NeuroFovea metamer model that is based on a mixture of peripheral representations and style transfer forward-pass algorithms for *any* image from the recent work of Adaptive Instance Normalization (Huang & Belongie). Our model is parametrized by a VGG-Net versus a set of joint statistics of complex wavelet coefficients which allows us to encode images in high dimensional space and interpolate between the content and texture information. We empirically show that human observers discriminate our metamers at a similar rate as the metamers of Freeman & Simoncelli (FS). In addition, our NeuroFovea metamer model gives us the benefit of near real-time generation which presents a $\times 1000$ speed-up compared to previous work. Critically, psychophysical studies show that both the FS and NeuroFovea metamers are discriminable from the original images highlighting an important limitation of current metamer generation methods.

1 Introduction

The history of metamers originally started through color matching theory, where two light sources were used to match another wavelength test, until both light sources are indistinguishable from each other producing what is called a *color metamer*. This leads us to define the general concept of metamer stimulus: two physically different stimuli that are perceptually equivalent [7, 36]. Freeman and Simoncelli [7] were the first to create such metamer stimuli through texture matching [3, 28] algorithms that tile the entire visual field locally given log-polar pooling regions that simulate the V1 and V2 receptive field sizes, as well as having global image statistics that match the metamer with the original image. The essence of their algorithm is to use gradient descent to match the global and tiled local texture statistics of an image (Portilla & Simoncelli [28]) given a fixation point with the original image until convergence. The computational complexity of their metamer synthesis algorithm is $O(MN)$, where M is the number of pooling regions, and N is the number of gradient descent steps per pooling region. See Figure 1 for an example of the metamers conditioned on point of fixation created by Freeman and Simoncelli.

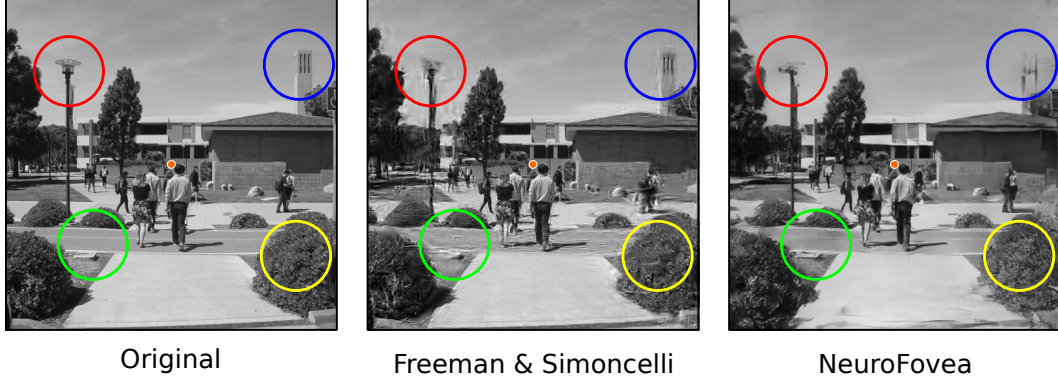


Figure 1: Comparison between metameric renderings. All three images are metameric to each other when they subtend a 26deg viewing angle, and when fixating at the center (orange dot). Four colored circles show different types of scrambling allowed at multiple eccentricities, contingent on the texture parameters of each model. Figure better viewed when zoomed in.

Despite the high quality metameric outputs, there are two current issues regarding metamer rendering. The first is that there exists a family of metamers that satisfy our previous definition such that there is no unique solution. Consider the trivial examples of having an image I and its metamer Q where all pixel values are identical except for one which is set to zero (making this difference unnoticeable), or the case where the metameric response has an imperceptible equal perturbation across all pixels [17, 7], such that $0 < |Q_i - I_i| < \epsilon, \forall$ pixels i (similar to the concept of Just Noticeable Differences [26, 5]). However, like the work of Freeman and Simoncelli and Rosenholtz *et al.* [19, 30, 2], we are interested in creating point-of-fixation driven metamers (or mongrels), which create images that preserve information in the fovea, yet lose spatial information in the periphery (through scrambling) such that this information is unnoticeable at a given fixation (Figure 1). The second issue is that the current state of the art for a complete field of view rendering of a $512\text{px} \times 512\text{px}$ metamer is 6 hours for a grayscale image and roughly a day for a color image. Moreover, the previous method produces errors when the image matrix is non-invertible (consider a black patch of all zeros).

From a theoretical standpoint, understanding how metamers can be created through deep models (VGG-Net) [33], may enable better understanding of what is encoded in the human visual system. Moreover, metameric visualizations may allow us to understand peripheral processing: what is the role of peripheral processing [29]? Can the peripheral nature of the human visual system give advantages to computer vision [6]? Constructing such models may also be used to emulate improved models of visual search [6, 30] and saliency [20, 4].

From a practical perspective, creating alternative metamers that are quick to compute may lead to the creation of rich neuroscience-driven experiments that require metameric stimuli such as gaze-contingent displays, or metameric videos for fMRI, EEG, MEG or Eye-Tracking [30] studies.

2 Previous Work

Recent work in texture synthesis through CNN's by Gatys *et al.* [10, 11] has lead to the development of a new popular subfield in the computer vision community called *Style Transfer* [34, 17, 15]: where an application of the texture synthesis algorithm can be used to transfer such textures onto the content of an image, hence 'transferring artistic style'. This parametric model uses per-layer Gram matrices that are computed with feature map activations pre-trained on ImageNet [32] when performing a forward pass of a texture. The idea is that the VGG-Net [33] which has been pre-trained for object classification can roughly represent the entire human visual stream simulated through the network, since it has hierarchically encoded object information in its layers [10, 11].

Despite the excellent texture synthesis results of Gatys *et al.*, their $O(N)$ algorithm is still limited by the N gradient descent steps that it must perform similar to the work of Portilla & Simoncelli [28], except that the features are driven by a VGG-Net CNN rather than a set of statistical parameters extracted from a steerable pyramid decomposition with the goal of fully describing the texture under the Julesz conjecture [18]. The latter proposing that any texture can be described by matching its n -th order statistics. This $O(N)$ performance bottleneck was solved through feed forward models

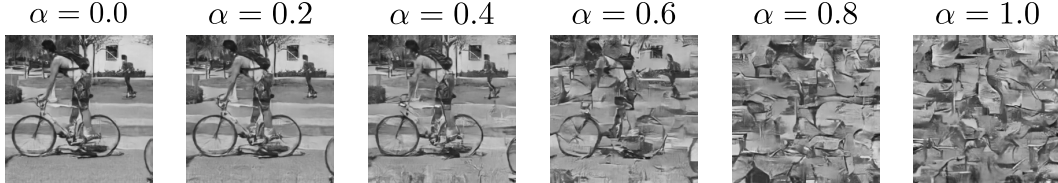


Figure 2: Interpolating between an image’s intrinsic content and texture via a convex combination in the output of the VGG-Net Encoder [33, 15]. Here we are treating the patch as a single pooling region. In our model, this interpolation given Eq. 1 is done for every pooling region in the visual field.

(Ulyanov et al; Johnson et al.) [34, 17] which can synthesize textures and perform style transfer in $O(1)$ time with high quality results. Their approach: rather than fixing the network and learning the image [10, 11], these feedforward models fix the image and essentially learn the texture and style parameters in the network through supervised training with texture and perceptual loss functions. However both models are limited to a single texture or style. The most recent work of Ming et al. [24] can also adapt feed forward synthesis and style transfer to a gamma of textures with a *single* network through a texture controller module, but can not adapt to unseen styles or textures. However the network is able to effortlessly blend multiple textures it has been trained on.

Gatys et al. [12] recently introduced guidance channels to control for perceptual style factors such as spatial control, color control and scale control. Their mathematical formulation is both applicable for Neural Style Transfer [11] (parametric matching through gradient descent) and Fast Neural Style Transfer [17] (feed-forward networks), however the network is constrained to only one style, and would have to be re-trained for any new style unseen in training.

Ideally, we would want a complete and flexible framework where a *single* network can encode *any* style and texture without the need to re-train, and with the power of producing style transfer with a single forward pass, thus enabling real-time applications. Furthermore, we would want such framework to also control for spatial and scale factors [12] which is critical in metamer rendering given the underlying peripheral architecture [2, 7, 1, 6, 19]. The very recent work of Huang and Belongie [15], enables such power through adaptive instance normalization(AdaIN), where an image is stylized by adjusting the mean and standard deviation of the *relu1_1*, *relu2_1*, *relu3_1*, *relu4_1* activations of the content image to match those of the style. Their framework also allows for spatial control [12]. However their model is currently adapted to a single binary window for spatial control of foreground vs background style transfer. Extending style transfer algorithms to work with M windows has been explored in Deep Photo Style Transfer [25] where Luan *et al.* have successfully created incredible photorealistic style transfer by mixing S different styles with M windows, however they reduce any sort of texture transfer by constraining the optimization with a ‘photorealism’ regularizer which avoids texturized distortions through an affine color transformation [23].

Other related work is of Deza & Eckstein [6] where they stack V1 peripheral architectures on top of dense clutter representations to produce foveated cluttered models [31, 38, 37, 27]. They show that such foveated versions predict target detectability better than dense versions, under forced fixation experiments. Along the same lines, we stack a V2 peripheral architecture [39, 8] on top of style transfer models (in their feature space through spatial control) [12] to create a foveated style transfer model. We show that a family of metamers can be produced through foveated style transfer. At the time of submission this is the first type of foveated style transfer model currently available (See Discussion, for parallel work). Technical aspects of our model will be discussed in the next Section.

3 Constructing the NeuroFovea metamer

To construct our metamer we propose the following statement: A metamer Q can be rendered by transferring M *localized* styles over a content image I , controlled by a set of style-to-content ratios α_i for every pooling region i . Every stylized location matches a pooling region as a function of eccentricity and receptive field size. We pick our receptive field sizes that match V2 [7] since it is strongly suggested that the size of such receptive fields encodes texture information [8, 39].

More formally: An input image $I \in \mathbb{R}^L$ is fed through a VGG-Net encoder [33] $\mathcal{V}(\cdot) : \mathbb{R}^L \rightarrow \mathbb{R}^D$ which is both the content and the style image, to produce the content feature $\mathbf{C} \in \mathbb{R}^D$, as shown in Figure 3. A noise patch $\mathcal{N} \sim (\mu_I, \sigma_I^2) \in \mathbb{R}^L$ is also fed through the same VGG-Net encoder producing the noise

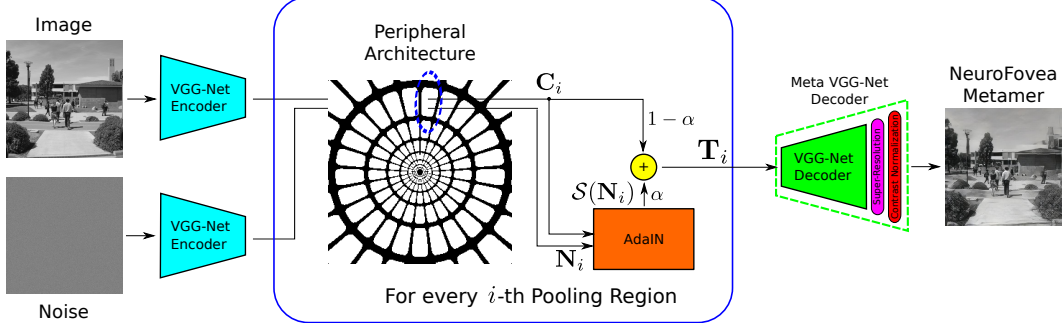


Figure 3: The NeuroFovea metamer generation schematic: An input image and a noise patch are fed through a VGG-Net encoder into a new feature space. Through spatial control [12] we can produce an interpolation for each pooling region [6] in such feature space between the stylized-noise (texture), and the content (the input image) [15]. This is how we successfully impose both global image and local texture-like constraints in every pooling region [7]. The metamer is the output of the pooled (and interpolated) feature vector through the Meta VGG-Net Decoder.

feature $\mathbf{N} \in \mathbb{R}^D$. These vectors are masked through spatial control [12], and the noise is stylized $\mathcal{S}(\cdot) : \mathbb{R}^D \rightarrow \mathbb{R}^D$ with the content which encodes a texture in the feature space through Adaptive Instance Normalization (AdaIN) [15]. A target feature $\mathbf{T}_i \in \mathbb{R}^D$ is defined as an interpolation between the stylized noise $\mathcal{S}(\mathbf{N}_i)$ and the content \mathbf{C}_i , in the feature space \mathbb{R}^D for every i -th pooling region:

$$\mathbf{T}_i(I, \alpha) = (1 - \alpha)\mathbf{C}_i(I) + \alpha\mathcal{S}(\mathbf{N}_i(I)) \quad (1)$$

In other words, we are finding an intermediate representation (the convex combination) between two vectors in \mathbb{R}^D . This concept is similar to the style-vs-content tradeoff, except that we are doing an image-vs-texture tradeoff, since the style and the content image are the same¹. Here we are interpolating along a straight-line which is the geodesic in \mathbb{R}^D , but this idea can produce other kinds of interpolations if we choose to constrain the interpolation to geodesics along some natural image manifold. This simple yet critical insight is the crux of our contribution in this paper. The final target feature vector \mathbf{T} is the masked sum of every \mathbf{T}_i with spatial control [12]. The metamer is the output of the Meta VGG-Net decoder [15] on \mathbf{T} , where the decoder receives only *one* vector and produces a global output rather than producing M outputs and stitching them together with cosine profiling functions.

Our Meta VGG-Net Decoder compensates for small artifacts by adding a *pix2pix* [16] Super-Resolution module which was trained on the Encoder-Decoder outputs to map to the original high resolution image. We then add a final global contrast image correction post-processing step. The correction is computed across the entire image, given the global mean and variance of the input image. Our pilot experiments agree with those done by Wallis *et al.* [36] which show that observers are quite sensitive to very subtle changes in contrast, even under matching texture parameters [28] in the periphery. Figure 3 fully describes our model.

The computational cost of our algorithm is $O(M)$, yet computing each metamer takes less than one second. Creating a single feed-forward neural architecture with engrained M -window spatial control is not the focus of our work. Note that such pipeline would be impressive since it would enable $O(1)$ metamer rendering via our framework. However, having an $O(M)$ model that is still reasonable to compute in less than a second gives us the flexibility of simulating multiple points of fixation, given that adjusting the point of fixation results in changing the location of the M pooling windows.

Additional specifications of our model: we use $M = M_p + M_f = 126$ spatial control windows, $M_p = 125$ pooling regions and $M_f = 1$ fovea (at an approximate 2deg radius). Details regarding the decoder network architecture and training can be seen in Huang *et al.* [15]. Constructions of biologically-tuned peripheral representations are explained in detail in [7, 1, 6]. Our *pix2pix* Super-Resolution module took 3 days to train on a Titan X GPU, and was trained with 64 crops (256×256) per image for 100 images, including horizontally mirrored versions. We ran 200 training epochs of these 12800 images

¹Also see Henaff & Simoncelli [14] for a similar idea of interpolating between two images along a geodesic.

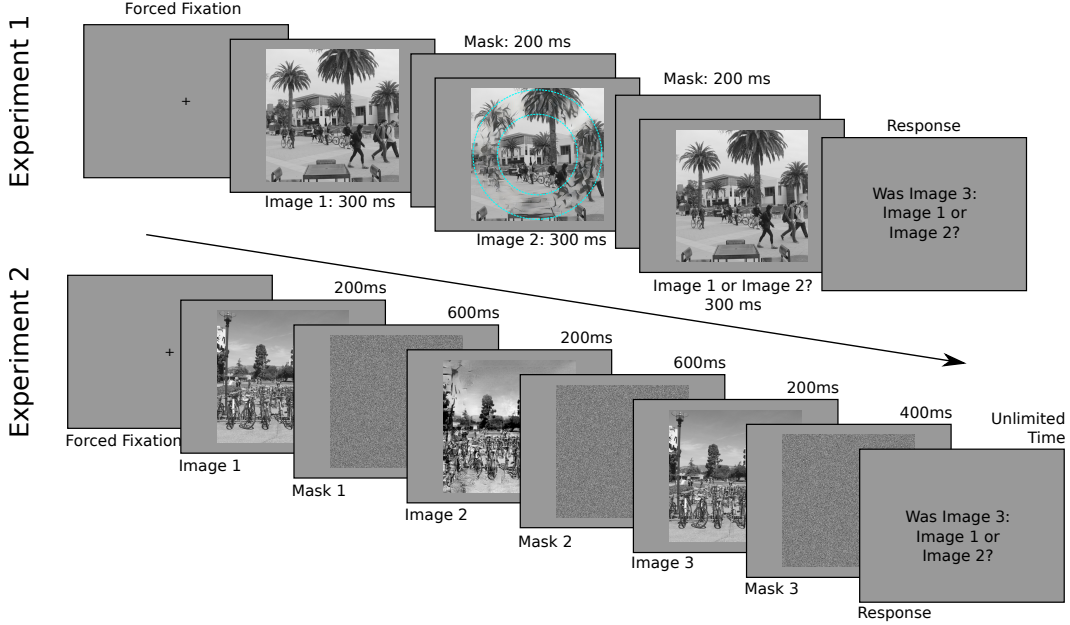


Figure 4: Experiment 1: Maximum Noise Estimation via Eccentricity Control (Top). The aim of this experiment is to see how susceptible are human observers towards distortions at different eccentricities that match the size of V2 receptive fields. The rings have been marked in cyan only in the figure for illustrative purposes. Experiment 2: Maximum Noise Estimation via Global Control (Bottom). The aim of this experiment is to benchmark our NeuroFovea model with different α values, and to compare it to the performance of Freeman and Simoncelli metamers.

on the U-Net architecture proposed by *Isola et al.* [16] which preserves local image structure as much as possible given an adversarial and L2 loss.

4 Methods

In the following Section we describe the experiments to assess whether our proposed technique generates metameric samples.

Six undergraduate observers (3 female) with 20/20 natural and corrected vision participated in all our experiments. All experiments were done with at a viewing distance of 52cm, and a 800×600 px resolution monitor, where each 512×512 image subtended $26\text{deg} \times 26\text{deg}$, as in the original experiments of Freeman and Simoncelli [7]. We used a BARCO monitor that was linearly calibrated to a mean luminance of 55.6 cd/m^2 . An SR-Research EyeLink 1000 Tower Mount with a refresh rate of 250 Hz was used to collect data for each experiment. Every observer went through a 9-point calibration before each session. Each condition in Experiment 1 was completed in roughly 2 hours on average, while Experiment 2 was completed in 3 hours. Both conditions in Experiment 1 had 1400 trials with 50 different images, while both conditions in Experiment 2 had 1800 trials with 100 different images. PsychToolbox for MATLAB was used to conduct our psychophysical experiments.

All our experiments were ABX tasks under a Forced-Fixation viewing condition at the center of the screen (observers are not allowed to move their eyes), and trials were discarded when observers broke center fixation. Figure 4 shows the schematic of an ABX task: Observers are shown two images: Image 1 and Image 2, each one masked after the other. Then a third image is shown: Image 3, and observers must guess if Image 3 is Image 1 or Image 2. Observers pressed the ‘a’ key to select Image 1, and the ‘l’ key to select Image 2. Experiment 1 had inter-stimulus masks, while Experiment 2 had inter-stimuli white noise masks to penalize small spatial distortions. They had unlimited time for response, but they all responded roughly in less than a second. If observers can’t discriminate between both images, their behavioural response will be at chance (50%), thus providing metameric evidence between both stimuli under forced fixation [7, 6]. Also see Wallis *et al.* [36] for alternative tests of local metamericism through an odd-ball paradigm.

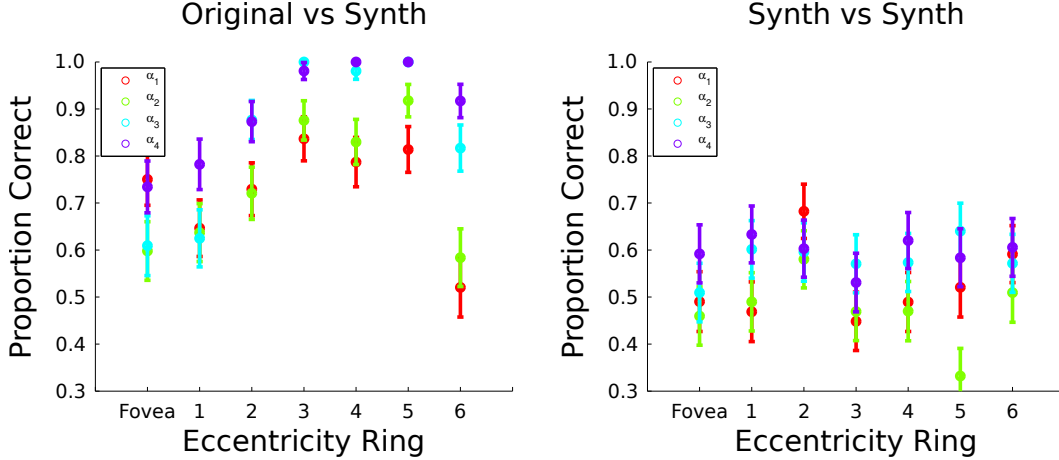


Figure 5: Experiment 1 shows how sensitive observers are to content-vs-texture tradeoffs at *any* eccentricity ring even when having the original image as background, compared to synthesized images. The drop at the farthest eccentricity is an artifact of showing square instead of round images.

5 Experiments

What is the maximum amount of distortion that is allowed in the visual periphery before an observer will notice? To address this question we look for a set of α values that will limit the amount of global structure loss vs texture loss for human observers (See Eq. 1). This is the main parameter for our model, *vs* the Freeman & Simoncelli model that varied a receptive field scaling factor (s), and also computed a closed-form expression psychometric function that would model such behavioural response parametrized by s . We will fix the scale ($s = 0.5$), to match the receptive field sizes of V2, and instead modify α . Note that finding the optimal α is non-trivial, as we do not know a priori the shape of the function $\alpha_i = \gamma_i(x)$, that will control how much noise (given our model parameters) is maximally allowed at each eccentricity x for the fully rendered image to be metamerич with the original.

For both our experiments we use the same 6 participants to engage in a series of ABX tasks where we randomly counterbalance two conditions:

1. Discriminating between Synthesized images (Synth vs Synth) which has been done in the original study of Freeman & Simoncelli. While this test does not guarantee metamerism (Original vs Synth), it is the evaluation the previous authors used for their experiments.
2. Discriminating between the Original and Synthesized images (Original vs Synth). This metamerism test, was not reported in previous works [7, 36].

These two conditions are similar to those proposed by Wallis *et al.* [36], however their study focused on discriminating local regions placed at multiple eccentricities within an image that have been replaced by purely synthesized textures without any global (image) constraints; i.e. texture-to-image [36] discrimination vs metamer-to-image discrimination (our study).

5.1 Experiment 1: Maximum Noise Estimation via Eccentricity Control

In our first experiment, we are interested in estimating what is the maximum amount of global loss that can be tolerated at multiple eccentricities in the periphery, with the hope of estimating these values independently, to consequently render a metamer with these different α_i values. An advantage of this method is that one can remain agnostic to the underlying $\gamma(\cdot)$ function that determines each α value for every eccentricity. The disadvantage of this method, is that one must do an exhaustive search of multiple α values per eccentricity to fully capture the point of subject equality. But most importantly: a theoretical drawback of this noise estimation process is that there is no guarantee that calculating eccentricity-driven α values will also be metamerич when all metamerич rings are stitched together; *i.e.*, it could be the case that *the whole is other than the sum of its parts* [21].

Nevertheless, any boundary estimation of α values will be useful when trying to compute global metamerism. We render metamerич rings at one of four possible noise values: $\alpha =$

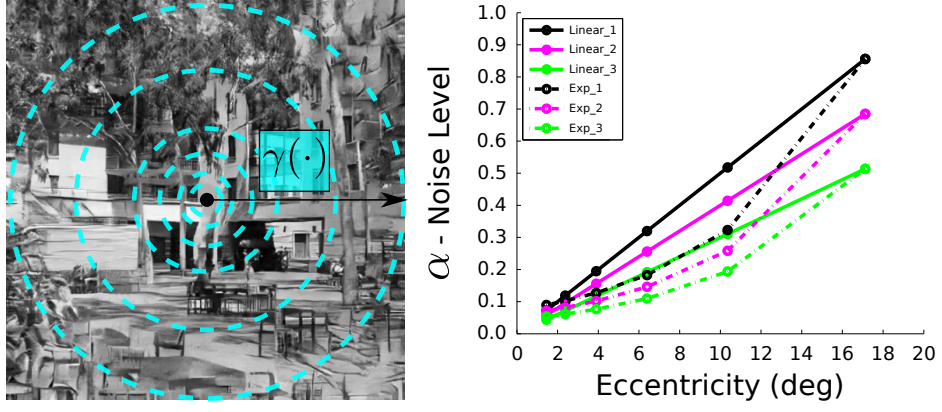


Figure 6: Left: Eccentricity ring boundaries are superimposed on the metamer in cyan to show how $\gamma(\cdot)$ modulates the image-to-texture tradeoff as a function of eccentricity. Right: A depiction of multiple $\gamma(\cdot)$ functions used to create metamer stimuli for Experiment 2.

$\{0.125, 0.375, 0.625, 0.875\}$, along 6 different eccentricities that match the receptive field size of V2. We also use the same noise values to test discrimination tolerance at the fovea. The metamer is blended with the background image (original or synth) through a cosine profiling function, such that at a given eccentricity only a metamer ring is perceived, while the remaining image is intact. Figure 4 (top) shows the schematic of Experiment 1.

Results: Figure 5 shows that observers do significantly well above chance when detecting distortions everywhere in the visual field, including the fovea. There is also a monotonic increase in proportion correct as eccentricity increases, but this is possibly due to the fact that greater eccentricities cover greater areas in the visual field [22]. The Synth vs Synth task shows that the bounds of the first eccentricity ring is: ($\alpha = 0.375$), and the second-to-largest in the periphery: ($\alpha = 0.875$). The rendered stimuli in this experiment did not use the Super-Resolution module, which suggests that even small artifacts can give away peripheral distortions. The significant difference in performance ($p < 0.05$) across all eccentricities including the fovea, also suggests that testing for metamerism in a Synth vs Synth task is a necessary but not sufficient condition for true metamerism [36].

5.2 Experiment 2: Maximum Noise Estimation via Global Control

In our second experiment we will evaluate global metamerism against synthetic image pairs, and against the original image. We explore this task for two main reasons: the first is to extend the results of Wallis *et al.* regarding the difficulty of discriminating original vs metamer stimuli – which consequently leads to explore if indeed true tests of metamerism via Synth vs Synth tasks are a necessary and sufficient condition. The second reason is to test the original metamers proposed by Freeman and Simoncelli [7] in a more rigorous environment (vs the original stimuli). If the results of the latter experiments are not at chance (*i.e.* there is *some* discriminability), this would imply that the Freeman & Simoncelli model does not hold for true metamerism [36].

We create a family of metamer stimuli rendered with multiple $\gamma(\cdot)$ curves. It would be naive to assume that metamers can only be produced by equally spaced α values along a linear function $\alpha_i = \gamma(x)$ as a function of eccentricity. Indeed, we do not know the shape of this function, which also depends on our choice of our image to texture interpolation as introduced in Eq. 1. We did not explore these mathematical constraints. Instead we render 6 families of metamers that obey either a linear function, or an exponential function, with 3 different parameters each. We build off the results of Experiment 1 to roughly estimate reasonable α -noise boundaries. In our first case: $\alpha_i = \gamma_i(x) = mx + b$, and in the second case: $\alpha_i = \gamma_i(x) = a \exp(bx)$; where x is the eccentricity of the i -th pooling regions in degrees of visual angle. All pooling regions that lie in the same ring, have the same α value. We call each curve *Linear_1*, *Linear_2*, *Linear_3* and *Exp_1*, *Exp_2*, *Exp_3* respectively, depending on their parameters as shown in Figure 6.

In addition, we have a base case condition (*Base_Case*) which is comparing the Meta Decoded image (including Super-Resolution and Contrast Normalization), without any noise, to test how well observers can discriminate minimal distortions given the invertibility of the AdaIN pipeline [15], as

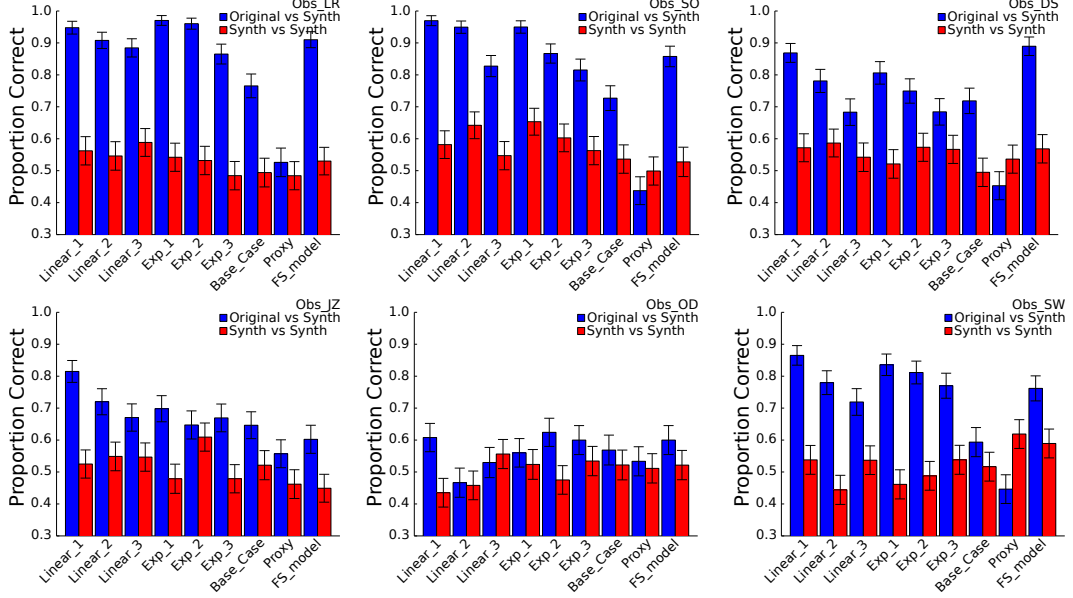


Figure 7: Results for multiple observers engaging in the two conditions of Experiment 2 across different metamer models: Original vs Synth and Synth vs Synth. Our NeuroFovea model with the $\gamma(\cdot)$ set to *Exp_3* produces metamers that rival those of Freeman and Simoncelli in both conditions.

well as a control condition (*Proxy*) which shows identical images in the ABX task. The theoretical and practical performance for this last condition should be 50% (chance). Finally, we also compare our NeuroFovea metamers to those of Freeman & Simoncelli [7] (*FS_model*), by selecting 50 images (not-cherry picked) from our dataset, and creating 2 metamer images of each one with the goal of inserting them in our final Original vs Synth and Synth vs Synth discriminability experiment. The previous model serves as a crucial baseline for metamerism.

Results: The results from our second experiment (Figure 7) show that all our NeuroFovea $\gamma(\cdot)$ functions produces similar behavioural responses to the metamers of Freeman and Simoncelli, with *Exp_3* and *Linear_3* showing a small comparative advantage. There was only a statistically significant advantage for the NeuroFovea for one observer. Four out of 6 observers showed significantly ($p < 0.05$) less discriminability between the *Base_Case* and the *FS_model*. This result seems to suggest that there might be more than one set of parameters that may achieve global metamerism (VGG-Net [33] vs Steerable Pyramid derived statistics [28]).

6 Discussion

The main difference of our method and that of Freeman & Simoncelli is that Freeman & Simoncelli used gradient descent to match local image appearance as well as texture statistics locally and globally for the image. Our method is performing an interpolation in VGG-Net space between the original image and the texturized version of the image (stylized noise in our model). Parallel work has investigated the use of different noise initializations such as matching power spectrum [9]. In addition, Parallel and complementary to our work: Wallis *et al.* have developed metamer images using gradient descent methods from the original NeuralSynth by Gatys *et al.*. However this model does not achieve metamerism between the original and synthetic images for all tested images [35] (only a subset). We have not tested if it the case that our model produces some group of metamer images given that we do not do our evaluations on a per image basis, but rather in the aggregate. However, it might be the case as our observers do not achieve near perfect discriminability in our original vs synth condition. See for example the performance of each observer in our *Exp_3* and *Base_Case* metamers, which fluctuates between 60% and 85% – an indication that observers are in fact confusing our metamers with the original images, but we have not evaluated if this is systematic for all observers. Moreover, each observer only evaluates each scene twice: once per condition (original vs synth, and synth vs synth).

A current limitation of each model is also the number of images they are evaluated with. The study of Freeman & Simoncelli use 4 images with an ABX task. The study of Wallis *et al.* [35] evaluates their set of images under an oddity paradigm [36], and our study uses 100 images under an ABX task with interstimuli white noise masks. Thus, metamerism should be tested on a wide variety of scenes that uniformly sample the scene manifold – as well as a wide variety of testing paradigms. Testing metamerism on a wide variety of scenes is of utmost importance given that metamerism for certain images that are heavily textured or uniform is easier to produce than a-periodic images or heavily cluttered [6] ones. Finding a subset of sufficient statistics [28, 33] that work for such images need not to apply for more complex scenes with less periodicity or clutter, which are still equally likely to appear in the real world.

Arguably, the most surprising finding of Experiment 2 is that neither the baseline (*Base_Case*) of our NeuroFovea model nor the Freeman & Simoncelli [7] model can generate images that are indistinguishable from the original images. This points to a severe limitation in all current methods.

However the central idea of our work and that of Freeman & Simoncelli [7], and recently Wallis *et al.* [35] remains: true metamerism may derive from capturing near-perfect image and texture statistics and interpolating (or matching [7, 35]) between them in a high dimensional feature space.

Future work in this direction may also explore the role of different layers of the VGG-Net for texture encoding: What layers are critical for metamerism and which ones are not? What is the minimum number of layers need to achieve metamerism through our pipeline? What network architectures are efficient towards encoding metamerism [13]? The parallel work of Funke *et al.* [9] has explored the role of texture matching via VGG-Net texture synthesis a la Gatys *et al.* (gradient descent), and has found that the third layer in a VGG-Net architecture is the minimal hierarchy for texture encoding in the periphery. This later finding supporting the use of our VGG-Net Decoder and Encoder architecture which includes layers up to *relu4_1*.

Indeed, generating metamers is still an open problem because of various constraints like human sensitivity to contrast levels and edges, statistical convergence of gradient descent rendering-based methods [11], and image rendering time. We have proposed a possible solution to this last problem via feed-forward style transfer techniques in our approach. Moreover, it is still not known what is the *minimum* set of parameters that both encode image content and texture across the entire visual field such that any small perturbation in these parameters will remove metamerism as first explored and mentioned by Freeman and Simoncelli.

7 Conclusion

In this paper we provide an innovative approach to utilize new methods in deep learning to try to generate metameristic images in real time. The proposed method based on style transfer (NeuroFovea model) matches that of Freeman & Simoncelli in the degree at which humans can discriminate between two synthetic images and also between the synthetic images and the original image. One advantage of the proposed method is that the metamers can be generated in near real time. Our psychophysical studies also point to a limitation of the two methods: humans can discriminate the rendered synthetic images from the originals. As style transfer research continues to move forward, we are confident that the core ideas of our model will be building blocks in constructing true visual metamers (original vs synthetic) that lie in the perceptual boundary of human discriminability.

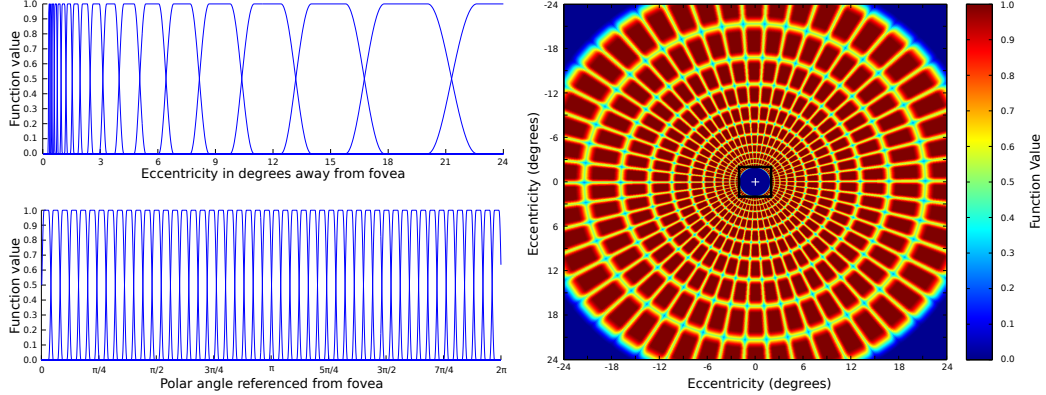
Acknowledgements

We would like to thank Xun Huang for sharing his code and valuable suggestions on AdaIN, Jeremy Freeman for making his metamer code available, Jamie Burkes for collecting original high-quality stimuli, N.C. Puneeth for insightful conversations on texture and masking, and Christian Bueno for informal lectures on homotopies. Mordechai Juni and Miguel Lago were also helpful in editing the manuscript and giving positive feedback. We would also like to thank NVIDIA for donating a Titan X GPU. This work was supported by the Institute for Collaborative Biotechnologies through grant 2 W911NF-09-0001 from the U.S. Army Research Office.

References

- [1] E. Akbas and M. P. Eckstein. Object detection through exploration with a foveated visual field. *arXiv preprint arXiv:1408.0814*, 2014.
- [2] B. Balas, L. Nakano, and R. Rosenholtz. A summary-statistic representation in peripheral vision explains visual crowding. *Journal of vision*, 9(12):13–13, 2009.
- [3] A. C. Bovik, M. Clark, and W. S. Geisler. Multichannel texture analysis using localized spatial filters. *IEEE transactions on pattern analysis and machine intelligence*, 12(1):55–73, 1990.
- [4] Z. Bylinskii, A. Recasens, A. Borji, A. Oliva, A. Torralba, and F. Durand. Where should saliency models look next? In *European Conference on Computer Vision*, pages 809–824. Springer, 2016.
- [5] S. J. Daly. Visible differences predictor: an algorithm for the assessment of image fidelity. In *SPIE/IS&T 1992 Symposium on Electronic Imaging: Science and Technology*, pages 2–15. International Society for Optics and Photonics, 1992.
- [6] A. Deza and M. Eckstein. Can peripheral representations improve clutter metrics on complex scenes? In *Advances In Neural Information Processing Systems*, pages 2847–2855, 2016.
- [7] J. Freeman and E. P. Simoncelli. Metamers of the ventral stream. *Nature neuroscience*, 14(9):1195–1201, 2011.
- [8] J. Freeman, C. M. Ziemba, D. J. Heeger, E. P. Simoncelli, and J. A. Movshon. A functional and perceptual signature of the second visual area in primates. *Nature neuroscience*, 16(7):974–981, 2013.
- [9] C. Funke, T. Wallis, A. Ecker, L. Gatys, F. Wichmann, and M. Bethge. A parametric texture model based on deep convolutional features closely matches texture appearance for humans. *Vision Sciences Society (VSS) Abstract*, 2017.
- [10] L. Gatys, A. S. Ecker, and M. Bethge. Texture synthesis using convolutional neural networks. In *Advances in Neural Information Processing Systems*, pages 262–270, 2015.
- [11] L. A. Gatys, A. S. Ecker, and M. Bethge. Image style transfer using convolutional neural networks. In *Proceedings of the IEEE Conference on Computer Vision and Pattern Recognition*, pages 2414–2423, 2016.
- [12] L. A. Gatys, A. S. Ecker, M. Bethge, A. Hertzmann, and E. Shechtman. Controlling perceptual factors in neural style transfer. *arXiv preprint arXiv:1611.07865*, 2016.
- [13] R. Geirhos, D. Janssen, H. Schutt, M. Bethge, and F. Wichmann. Of human observers and deep neural networks: A detailed psychophysical comparison. *Vision Sciences Society (VSS) Abstract*, 2017.
- [14] O. J. Hénaff and E. P. Simoncelli. Geodesics of learned representations. *arXiv preprint arXiv:1511.06394*, 2015.
- [15] X. Huang and S. Belongie. Arbitrary style transfer in real-time with adaptive instance normalization. *arXiv preprint arXiv:1703.06868*, 2017.
- [16] P. Isola, J.-Y. Zhu, T. Zhou, and A. A. Efros. Image-to-image translation with conditional adversarial networks. *arXiv preprint arXiv:1611.07004*, 2016.
- [17] J. Johnson, A. Alahi, and L. Fei-Fei. Perceptual losses for real-time style transfer and super-resolution. In *European Conference on Computer Vision*, pages 694–711. Springer, 2016.
- [18] B. Julesz. Textons, the elements of texture perception, and their interactions. *Nature*, 290(5802):91–97, 1981.
- [19] S. Keshvari and R. Rosenholtz. Pooling of continuous features provides a unifying account of crowding. *Journal of Vision*, 16(39), 2016.
- [20] K. Koehler, F. Guo, S. Zhang, and M. P. Eckstein. What do saliency models predict? *Journal of vision*, 14(3):14–14, 2014.
- [21] K. Koffka. *Principles of Gestalt psychology*, volume 44. Routledge, 2013.
- [22] A. M. Larson and L. C. Loschky. The contributions of central versus peripheral vision to scene gist recognition. *Journal of Vision*, 9(10):6–6, 2009.
- [23] A. Levin, D. Lischinski, and Y. Weiss. A closed-form solution to natural image matting. *IEEE Transactions on Pattern Analysis and Machine Intelligence*, 30(2):228–242, 2008.
- [24] Y. Li, C. Fang, J. Yang, Z. Wang, X. Lu, and M.-H. Yang. Diversified texture synthesis with feed-forward networks. *arXiv preprint arXiv:1703.01664*, 2017.
- [25] F. Luan, S. Paris, E. Shechtman, and K. Bala. Deep photo style transfer. *arXiv preprint arXiv:1703.07511*, 2017.
- [26] J. Lubin. A human vision system model for objective picture quality measurements. In *Broadcasting Convention, 1997. International*, pages 498–503. IET, 1997.

- [27] A. Oliva, M. L. Mack, M. Shrestha, and A. Peeper. Identifying the perceptual dimensions of visual complexity of scenes.
- [28] J. Portilla and E. P. Simoncelli. A parametric texture model based on joint statistics of complex wavelet coefficients. *International Journal of Computer Vision*, 40(1):49–70, 2000.
- [29] R. Rosenholtz. Capabilities and limitations of peripheral vision. *Annual Review of Vision Science*, 2:437–457, 2016.
- [30] R. Rosenholtz, J. Huang, A. Raj, B. J. Balas, and L. Ilie. A summary statistic representation in peripheral vision explains visual search. *Journal of vision*, 12(4):14–14, 2012.
- [31] R. Rosenholtz, Y. Li, J. Mansfield, and Z. Jin. Feature congestion: a measure of display clutter. In *Proceedings of the SIGCHI conference on Human factors in computing systems*, pages 761–770. ACM, 2005.
- [32] O. Russakovsky, J. Deng, H. Su, J. Krause, S. Satheesh, S. Ma, Z. Huang, A. Karpathy, A. Khosla, M. Bernstein, et al. Imagenet large scale visual recognition challenge. *International Journal of Computer Vision*, 115(3):211–252, 2015.
- [33] K. Simonyan and A. Zisserman. Very deep convolutional networks for large-scale image recognition. *arXiv preprint arXiv:1409.1556*, 2014.
- [34] D. Ulyanov, V. Lebedev, V. Lempitsky, et al. Texture networks: Feed-forward synthesis of textures and stylized images. In *Proceedings of The 33rd International Conference on Machine Learning*, pages 1349–1357, 2016.
- [35] T. Wallis, C. Funke, A. Ecker, L. Gatys, F. Wichmann, and M. Bethge. Towards matching peripheral appearance for arbitrary natural images using deep features. *Vision Sciences Society (VSS). Abstract*, 2017.
- [36] T. S. Wallis, M. Bethge, and F. A. Wichmann. Testing models of peripheral encoding using metamerism in an oddity paradigm. *Journal of vision*, 16(2):4–4, 2016.
- [37] C.-P. Yu, W.-Y. Hua, D. Samaras, and G. Zelinsky. Modeling clutter perception using parametric proto-object partitioning. In *Advances in Neural Information Processing Systems*, pages 118–126, 2013.
- [38] C.-P. Yu, D. Samaras, and G. J. Zelinsky. Modeling visual clutter perception using proto-object segmentation. *Journal of vision*, 14(7):4–4, 2014.
- [39] C. M. Ziemba, J. Freeman, J. A. Movshon, and E. P. Simoncelli. Selectivity and tolerance for visual texture in macaque v2. *Proceedings of the National Academy of Sciences*, 113(22):E3140–E3149, 2016.



(a) Top: $g_n(e)$ function. Bottom: $h_n(\theta)$ function.

(b) Peripheral Architecture.

Figure 8: Construction of a Peripheral Architecture *a la* Freeman & Simoncelli [7] using the functions described in this section are shown in Fig. 8(a). The blue region in the center of Fig. 8(b), represents the fovea where all information is preserved. Outer regions (in red), represent different parts of the periphery at multiple eccentricities. Original figure from Deza & Eckstein [6].

8 Supplementary Material

8.1 Creation of Peripheral Architecture

In our work we use a V2 peripheral architecture which presents a scaling factor s of ($s = 0.5$) as proposed in Freeman & Simoncelli which is the maximum scaling factor used for metameristic perception given Portilla & Simoncelli texture parameters. The V1 peripheral architecture model [6, 7] which pools over lower level features such as Feature Congestion [31] is set to a scaling factor of $s = 0.25$. The scaling factor controls the rate of growth of the pooling regions in the visual field, which in return will control how much scrambling or crowding occurs per pooling region. More specifically: $w_\theta = s/2$ and $N_\theta = 2\pi/w_\theta$. Equations 2 3 4 fully describe these log-polar regions (Fig. 8).

$$f(x) = \begin{cases} \cos^2\left(\frac{\pi}{2}\left(\frac{x-(t_0-1)/2}{t_0}\right)\right); & -(1+t_0)/2 < x \leq (t_0-1)/2 \\ 1; & (t_0-1)/2 < x \leq (1-t_0)/2 \\ -\cos^2\left(\frac{\pi}{2}\left(\frac{x-(1+t_0)/2}{t_0}\right)\right) + 1; & (1-t_0)/2 < x \leq (1+t_0)/2 \end{cases} \quad (2)$$

$$h_n(\theta) = f\left(\frac{\theta - (w_\theta n + \frac{w_\theta(1-t_0)}{2})}{w_\theta}\right); w_\theta = \frac{2\pi}{N_\theta}; n = 0, \dots, N_\theta - 1 \quad (3)$$

$$g_n(e) = f\left(\frac{\log(e) - [\log(e_0) + w_e(n+1)]}{w_e}\right); w_e = \frac{\log(e_r) - \log(e_0)}{N_e}; n = 0, \dots, N_e - 1 \quad (4)$$

8.2 Example Stimuli in Experiments

Figures 9 and 10 show some of the stimuli used in our experiments, where better comparisons can be made between the different the original image and our Metameristic outputs (Exp_1, Exp_2, Exp_3, Linear_1, Linear_2, Linear_3, Base_Case), as well as the NeuroFovea. Scrambling in the outer periphery is quite noticeable for Exp_1 and Linear_1, while Exp_3 and Linear_3, show smoother transitions of image-to-texture interpolation across the visual field. The Base_Case inversion can also be observed, where indeed a very close approximation to the original image is achieved, yet even under this baseline condition human observers are quite susceptible to small distortions, local contrast differences, or possibly the loss of high-spatial frequency information of the image.

What also remains to be evaluated in experiments regarding visual metamerism is the role of attention when evaluating across images. Freeman and Simoncelli evaluated to control for such factors by extending stimuli presentation time, as well as endogenous cues that signal the area of greatest difference between synthesized examples [7]. How do landmarks affect metameristic perception? How can we classify a priori, both semantically and computationally what makes an image difficult to metamerize? What attentional strategies do observers use to improve their discriminability of the images in the ABX task, or is this due purely to perceptual variance across subjects? These are all important questions that should be addressed in future work regarding metamerism and attention.

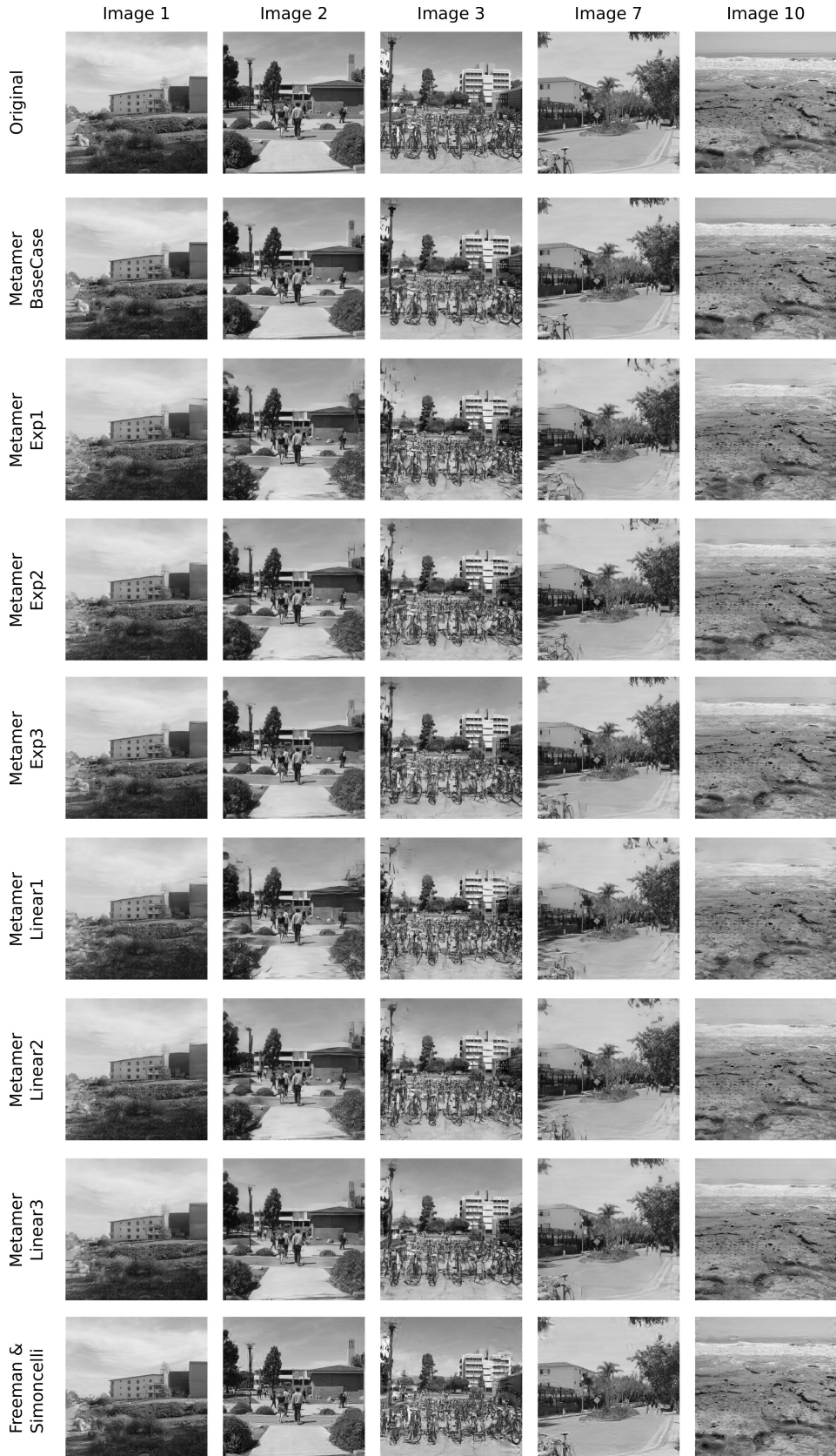


Figure 9: Five of the 100 images and their respective metamers used in our experiments. Images and distortions best viewed when zoomed in. Original stimuli were rendered at 512×512 px and 26×26 deg.

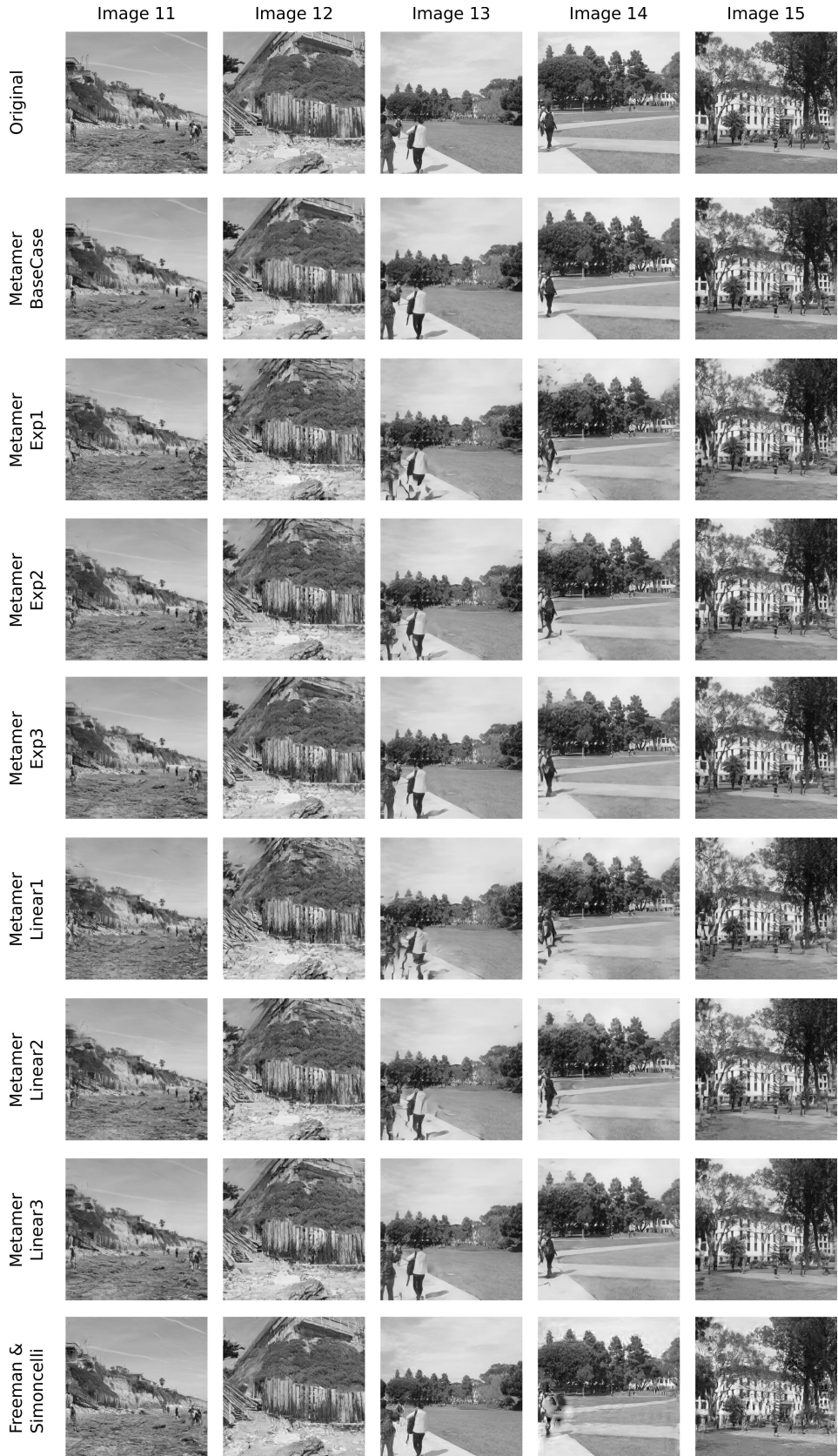


Figure 10: Five of the 100 images and their respective metamers used in our experiments. Images and distortions best viewed when zoomed in. Original stimuli were rendered at 512×512 px and 26×26 deg.